

# Effects of Damper Winding on Commutation of Commutatorless Motors

著者	Takeda Yoji, Hayashi Yasutsugu, Hirasa Takao
引用	Bulletin of University of Osaka Prefecture. Series A, Engineering and natural sciences. 1974, 22(2), p.121-129
URL	<a href="http://doi.org/10.24729/00008753">http://doi.org/10.24729/00008753</a>

# Effects of Damper Winding on Commutation of Commutatorless Motors

Yoji TAKEDA\*, Yasutsugu HAYASHI\*\* and Takao HIRASA\*

(Received November 15, 1973)

This report deals theoretically with effects of damper windings related to commutation characteristics on various kinds of commutatorless motor, such as the lapping angles and the allowable armature current limits, and describes the experimental results on three typical types of the motor in which the commutator elements are 1, 2 and 3 pairs. As the results, the allowable armature current limits are considerably increased by the  $q$ -axis damper winding for the 1 pair's motor, but for the 2 and 3 pairs' motor, the current limits are increased scarcely, consequently the  $q$ -axis damper winding is not so effective. The  $d$ -axis damper and field windings are able to improve remarkably the commutation characteristics for all the machine types.

## 1. Introduction

The most important problem of commutatorless motors using thyristor commutators instead of mechanical commutators on a DC motor is commutating actions of the thyristor commutators. On an induced voltage commutating system which depends on only counter *e. m. fs* as commutating power sources, the ability of the commutation is so small that the commutation failures are taken place on some driving conditions. In order to improve the commutating actions, the commutatorless motor commonly needs the damper windings.<sup>1)~4)</sup> In this paper, the effects of the damper windings on the over-lapping angle and the maximum allowable armature current are described.

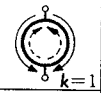
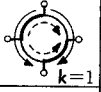
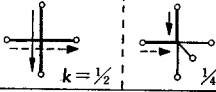
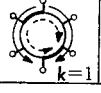
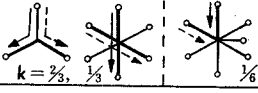
At first, the commutatorless motor can be classified into two great divisions according to the commutating action. One is provisionally named "reversal commutation" in which the direction of the current in the armature winding taking part in the commutation is reversed in the commutation period. The other is named "removal commutation" in which the armature current is removed from the conducting armature winding to the next winding. With a number of commutator elements  $n$  and an active armature winding coefficient  $k$  which is the ratio of the active armature windings in the commutating period to all the armature windings,<sup>5)</sup> each of equivalent circuits for two commutating systems is given, and then the generalized equations of the over-lapping angle and the allowable armature current limit are theoretically derived. At last, the experimental results on three typical types of the commutatorless motors are shown as compared with the theoretical ones.

\* Department of Electrical Engineering, College of Engineering.

\*\* Graduate Student, Department of Electrical Engineering, College of Engineering.

2. Commutating Systems

The various kinds of the commutatorless motor are shown in table 1.

Reversal commutation		Removal commutation	
$n$	Armature connection	$n$	Armature connection *
1		$\frac{3}{2}$	
2		2	
3		3	

\*Broad-pointed line shows the commutating armature winding from  $\rightarrow$  to  $\dashrightarrow$

Table. 1. Various kinds of commutatorless motor.

2.1 Reversal commutation

In this commutating system, all the armature windings are always conducting, therefore  $k$  is unity. As an example, the armature windings in the commutating period for  $n=3$  and  $k=1$  are shown in Fig. 1. The axis of the active armature winding  $A \rightarrow A'$  is shifted to the axis  $B \rightarrow B'$  by the switching actions in that period.

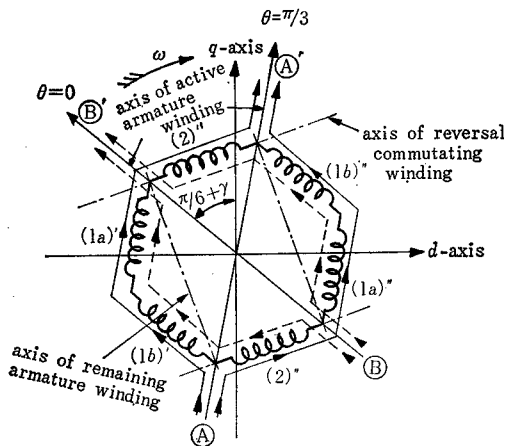


Fig. 1. Armature winding for reversal commutation.

The directions of the currents in the armature winding (2)' and (2)'' are reversed, but the currents in the remaining armature windings (1a)', (1b)' etc. are not changed. The armature windings that the currents are reversed are  $1/n$  of all the armature windings. The angles of the axes (1)' and (2)' are different by  $\pi/2$ . Consequently, the mutual inductance between them can not exist. The equivalent circuit of the

reversal commutation including the smoothing reactor is shown in Fig. 2. Arranging the two parallel windings (1)', (1)'' and (2)', (2)'' into one group, and removing the non-commutating winding (1) out of the thyristor bridge, Fig. 2 can be rewritten as Fig. 4(a).

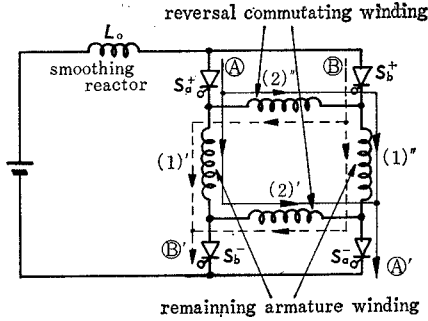


Fig. 2. Equivalent circuit on reversal commutation.

2.2 Removal commutation

As an example of this commutation, the armature windings for  $n=3$  and  $k=2/3$  are shown in Fig. 3 and Fig. 4(b). The armature current is removed from the conducting armature winding (3) to the other non-conducting winding (4). Consequently, all the armature windings are not always conducting, so that  $k$  is smaller than unity.

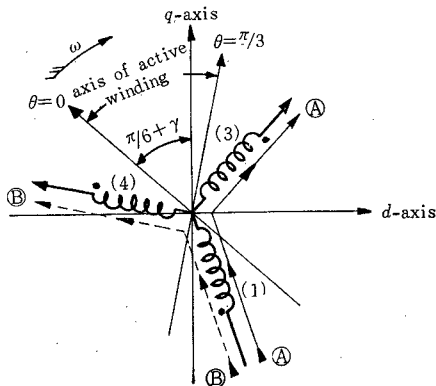


Fig. 3. Armature winding on removal commutation.

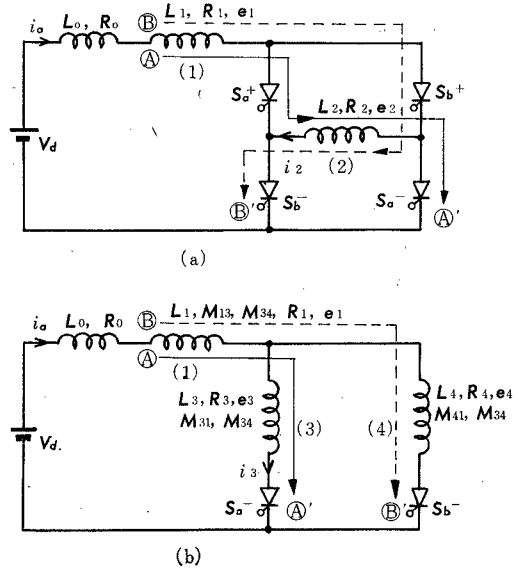


Fig. 4. Equivalent circuits of reversal and Removal commutation.

**3. Analyses of Commutation Characteristics**

**3.1 Reversal commutation**

In an over-lapping period all the thyristors are conducting in Fig. 4(a), the armature currents  $i_a(\theta)$  and  $i_2(\theta)$  are

$$i_a(\theta) = \frac{V_d}{R_{01}}(1 - \varepsilon^{-T_{01}\theta}) - \frac{E_1}{Z_{01}}[\cos(\theta + \beta_1 - \varphi_{01}) - \varepsilon^{-T_{01}\theta}\cos(\beta_1 - \varphi_{01})] + i_a(0)\varepsilon^{-T_{01}\theta} \dots\dots\dots(1)$$

$$i_2(\theta) = -\frac{E_2}{Z_2}[\cos(\theta + \beta_2 - \varphi_2) - \varepsilon^{-T_2\theta}\cos(\beta_2 - \varphi_2)] - i_a(0)\varepsilon^{-T_2\theta} \dots\dots\dots(2)$$

where,

$V_d$ ; the DC source voltage,

$\omega$ ; the angular velocity,

$\theta$ ; the angle in electrical unit,

$E_1$ ; the maximum value of the counter *e. m. f.*  $e_1$  of the armature winding (1),

$\beta_1$ ; the phase angle of  $e_1$  for the *q*-axis,

$E_2$ ; the maximum value of the counter *e. m. f.*  $e_2$  of the armature winding (2),

$\beta_2$ ; the phase angle of  $e_2$  for the *q*-axis,

$$R_{01} = R_0 + R_1, \quad L_{01} = L_0 + L_1, \quad T_{01} = R_{01}/\omega L_{01}, \quad \varphi_{01} = \tan^{-1}(\omega L_{01}/R_{01}).$$

$$T_2 = R_2/\omega L_2, \quad \varphi_2 = \tan^{-1}(\omega L_2/R_2)$$

At the end of the over-lapping period, the current equation is

$$i_a(u) = i_2(u) \dots\dots\dots(3)$$

where  $u$  is over-lapping angle.

Therefore, from eqs. (1), (2) and (3),

$$\left\{ \frac{E_1}{Z_1}[\cos(u + \beta_1 - \varphi_{01}) - \varepsilon^{-T_{01}u}\cos(\beta_1 - \varphi_{01})] - \frac{V_d}{R_{01}}(1 - \varepsilon^{-T_{01}u}) \right\} - \frac{E_2}{Z_2}[\cos(u + \beta_2 - \varphi_2) - \varepsilon^{-T_2u}\cos(\beta_2 - \varphi_2)] = i_a(0)(\varepsilon^{-T_{01}u} + \varepsilon^{-T_2u}) \dots\dots\dots(4)$$

In this equation, however, the value of the initial armature current  $i_a(0)$  is unknown and the commutating over-lapping angle  $u$  is included in the cosine and exponential terms. In order to get the value of  $u$  a method of trial and error is needed. Therefore, it is very difficult and troublesome to calculate  $u$ . For the easy analysis of  $u$ , the following assumptions are made,

1) The smoothing reactor has so large inductance that the armature current is enough smooth. Therefore,  $i_a(0)$  is equal to the average armature current  $I_a$ ,

2) As the armature inductance is much greater than the armature resistance, the first term of the left-hand side in eq. (4) can be neglected, and eq. (4) is replaced with the following equation,

$$\sin \beta_2 - \sin(u + \beta_2) = 2\omega L_2 I_a / E_2 \dots\dots\dots(5)$$

where,

$$\left. \begin{aligned} L_2 &= L_a \sin^2(\pi/2n) \\ E_2 &= \omega M_a I_f \sin(\pi/2n) \end{aligned} \right\} \dots\dots\dots(6)$$

$L_2$ ; the inductance of all the armature windings,

$I_f$ ; the field current

$M_{af}$ ; the armature inductance between the field and armature winding.

From eqs. (5) and (6), the over-lapping angle is given by

$$u = \sin^{-1} \left[ \sin \beta_2 - \frac{2L_a I_a \sin(\pi/2n)}{M_{af} I_f} \right] - \beta_2 \quad \dots\dots\dots(7)$$

The allowable armature current limit  $I_{amax}$  is the greatest value of  $I_a$  in eq. (5). But in eq. (5), the right-hand side term becomes the largest value at  $\sin(u + \beta_2) = -1$ , that is,

$$u = -\pi/2 - \beta_2 \quad \dots\dots\dots(8)$$

Substituting eqs. (6) and (8) into eq. (5), then

$$I_{amax} = \frac{M_{af} I_f}{2L_a \sin(\pi/2n)} (1 + \sin \beta_2) \quad \dots\dots\dots(9)$$

**3.2 Removal commutation**

Considering the boundary conditions of the armature currents, the current of the winding (3)  $i_3(\theta)$  is

$$\begin{aligned} i_3(\theta) = & \frac{V_a}{2R_{013}} (1 - \varepsilon^{-T_{013}\theta}) + (\varepsilon^{-T_3\theta} + \varepsilon^{-T_{013}\theta}) \frac{i_a(0)}{2} \\ & - \frac{E_{34}}{2Z_{013}Z_3} \left[ Z_{01} \cos(\theta + \beta_{34} - \varphi_{013} - \varphi_3 + \varphi_{01}) - Z_{013} \cos(\beta_{34} - \varphi_3) \varepsilon^{-T_3\theta} \right. \\ & \left. + \frac{Z_3}{2} \cos(\beta_{34} - \varphi_{013}) \varepsilon^{-T_{013}\theta} \right] - \frac{E_{13}}{2Z_{13}} [\cos(\theta + \beta_{13} - \varphi_{013}) \\ & - \cos(\beta_{13} - \varphi_{013}) \varepsilon^{-T_{013}\theta}] \quad \dots\dots\dots(10) \end{aligned}$$

where,

$$\begin{aligned} e_{34} &= e_3 - e_4 = E_3 \varepsilon^{j\beta_3} - E_4 \varepsilon^{j\beta_4} = E_{34} \varepsilon^{j\beta_{34}}, \\ e_{13} &= e_1 + e_3 = E_1 \varepsilon^{j\beta_1} + E_3 \varepsilon^{j\beta_3} = E_{13} \varepsilon^{j\beta_{13}}, \\ R_{013} &= R_0 + R_1 + R_3, \quad L_{013} = L_0 + L_1 + L_3, \quad Z_{013} = \sqrt{R_{013}^2 + (\omega L_{013})^2}, \\ T_{013} &= R_{013} / \omega L_{013}, \quad \varphi_{013} = \tan^{-1}(\omega L_{013} / R_{013}), \\ R_{01} &= R_0 + R_1, \quad L_{01} = L_0 + L_1, \quad \varphi_{01} = \tan^{-1}(\omega L_{01} / R_{01}), \\ T_3 &= R_3 / \omega L_3, \quad \varphi_3 = \tan^{-1}(\omega L_3 / R_3) \end{aligned}$$

$e_1, e_3$  and  $e_4$ ; the counter *e. m. fs.* of the armature winding (1), (3) and (4),

$\beta_1, \beta_3$  and  $\beta_4$ ; the phase angles of  $e_1, e_3$  and  $e_4$  for the *q*-axis.

As  $i_3(\theta)$  becomes zero at the end of the removal commutating period, the over-lapping angle  $u$  is solved from  $i_3(u) = 0$ . But in eq. (10), the initial current  $i_a(0)$  is unknown. Therefore, the analysis of  $u$  must be taken by the method of trial and error, as well as the reversal commutation. In order to get the approximate solution the same assumptions in the reversal commutation are made. Then eq. (10) is

$$\sin(u + \beta_{34}) - \sin \beta_{34} = 2\omega L(M)_3 I_a / E_{34} \quad \dots\dots\dots(11)$$

where,

$$\left. \begin{aligned} L(M)_3 &= L_3 - M_{34} = (1 - \sigma_{34} \cos \beta_{34}) L_a \sin^2(\pi/2n), \\ E_{34} &= |E_3(\varepsilon^{j\beta_3} - \varepsilon^{j\beta_4})| \\ &= |\omega M_{af} I_f \sin(\pi/2n) (\varepsilon^{j\beta_3} - \varepsilon^{j\beta_4})| \end{aligned} \right\} \quad \dots\dots\dots(12)$$

$M_{34}$ ; the mutual inductance between the windings (3) and (4),

$\sigma_{34}$ ; the coupling coefficient between the windings (3) and (4).

Over-lapping angle  $u$  is given from eq. (11)

$$u = \sin^{-1} \left[ \sin \beta_{34} + \frac{2(1 - \sigma_{34} \cos \beta_{34}) L_a I_a \sin(\pi/2n)}{M_{af} I_f (e^{j\beta_3} - e^{j\beta_4})} \right] - \beta_{34} \quad \dots\dots\dots(13)$$

and  $u$  for the allowable armature current limit can be obtained at the maximum value of  $\sin(u + \beta_{34})$  in eq. (11), that is,

$$u = \pi/2 - \beta_{34} \quad \dots\dots\dots(14)$$

Substituting eqs. (12) and (14) into eq. (11), then

$$I_{amax} = \frac{|M_{af} I_f (e^{j\beta_3} - e^{j\beta_4})|}{2(1 - \sigma_{34} \cos \beta_{34}) L_a \sin(\pi/2n)} (1 - \sin \beta_{34}) \quad \dots\dots\dots(15)$$

From eqs. (7), (9), (13) and (15), it is seen that the commutating characteristics depend on the inductance of the commutating armature winding.

**4. Effect of Damper Winding**

In order to improve the commutation characteristics, the armature inductance associated with the commutation must be made as small as possible. Decrease in the inductance brings decrease in the over-lapping angle and increase in the allowable armature current limit. Consequently, the damper windings are needed for above purpose, because the damper windings are able to decrease the commutating inductance. In this chapter, the effects of the damper windings are explained in association with the leading commutating angle. The positions of the commutating winding on the typical types of the commutatorless motor are shown in Fig. 5. The commutation is begun when the angle between the commutating windings' axis and the  $d$ -axis becomes  $\gamma$ . On the small leading commutating angle  $\gamma$ , the  $d$ -axis damper winding placed on the  $d$ -axis exerts a favourable influence upon the commutating inductance, and the  $q$ -axis damper winding has little influence upon it. But with the increase in  $\gamma$ , the inductance is more greatly influenced by the  $q$ -axis damper winding. Generally speaking, the field winding placed on the  $d$ -axis effectively acts as the  $d$ -axis damper winding and produces analogous effects<sup>6)</sup>. Consequently, the ordinary commutatorless motors have essentially the effects of the  $d$ -axis damper winding.

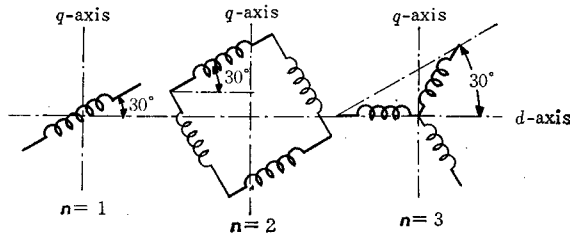


Fig. 5. Position of commutating armature winding at  $\gamma=30^\circ$ .

5. Experimental Results

On the experiments, two motors of same capacities and ratings and different types are employed. One has four salient poles without the damper winding, but the field winding produces the analogous effects of the *d*-axis damper winding. The other has the same poles with the *q*-axis damper winding. As a result, the one is with the *d*-axis damper winding and the other is with the both of *d*- and *q*-axis damper windings.

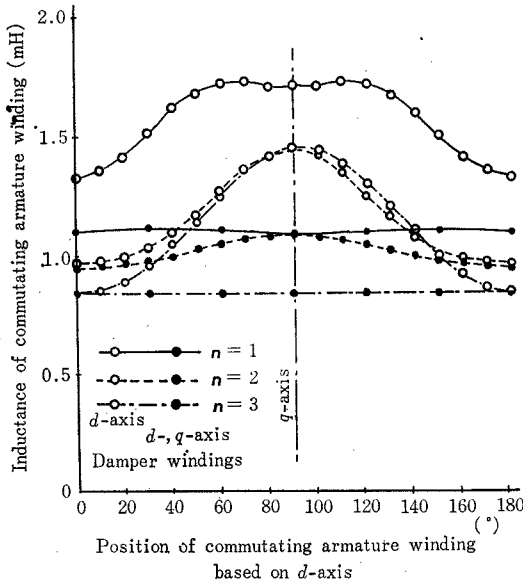


Fig. 6. Inductance of commutating armature winding.

The measured inductances of the armature winding are shown in Fig. 6. Care must be taken that the inductances with the *d*-axis damper winding are small at the *d*-axis and large at the *q*-axis. But, on the machine with the *d*- and *q*-axis damper

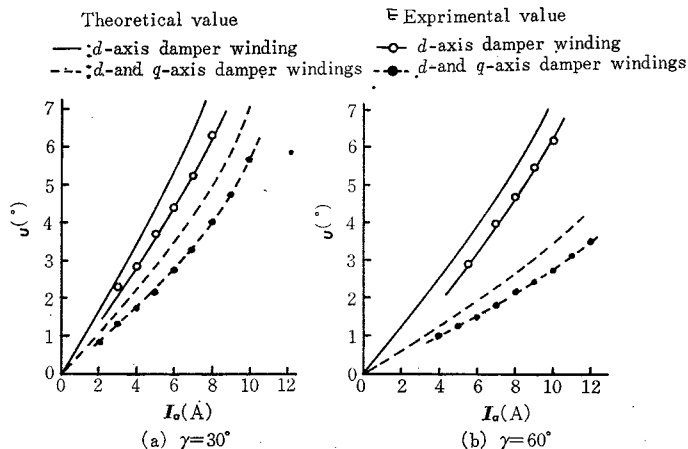


Fig. 7. Over-lapping angle v. s armature current.

windings, the inductances are reduced especially near the  $q$ -axis by the effect of the  $q$ -axis damper winding.

The experimental results of the over-lapping angle are shown in Figs. 7 and 8.

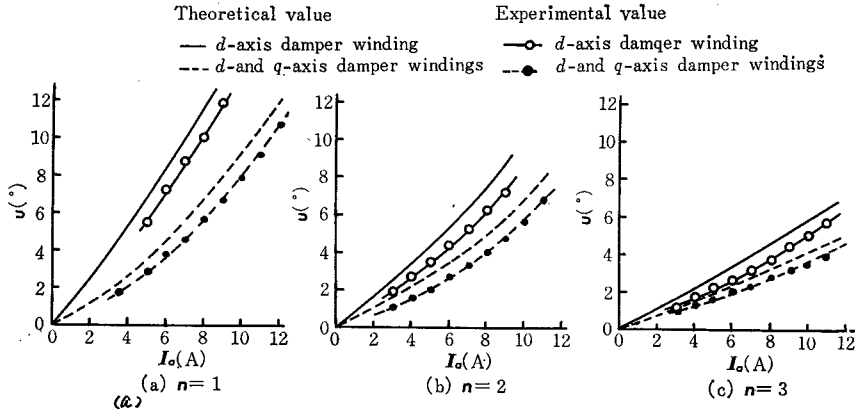


Fig. 8. Over-lapping angle  $v$ , s armature current.

There are considerable differences between the theoretical and experimental results. As the reason, it may be seen that the measured inductances are not necessarily exact values. There are, however, a similar tendency between them. The over-lapping angles are increased by the increase of the armature current and decreased by the increases of the commutator elements and the leading commutating angle.<sup>7),8)</sup> As mentioned above, the  $q$ -axis damper winding causes the decrease of the commutating inductance near the  $q$ -axis, so that the over-lapping angle for the  $d$ - and  $q$ -axis damper windings becomes smaller than that for only the  $d$ -axis damper winding, especially on the large leading commutating angle. This tendency becomes more remarkable with smaller  $n$  as shown in Fig. 8. Fig. 9 shows the allowable armature current limit. For  $n=2$  or 3, the allowable armature current limit for the  $d$ - and  $q$ -axis damper windings is little

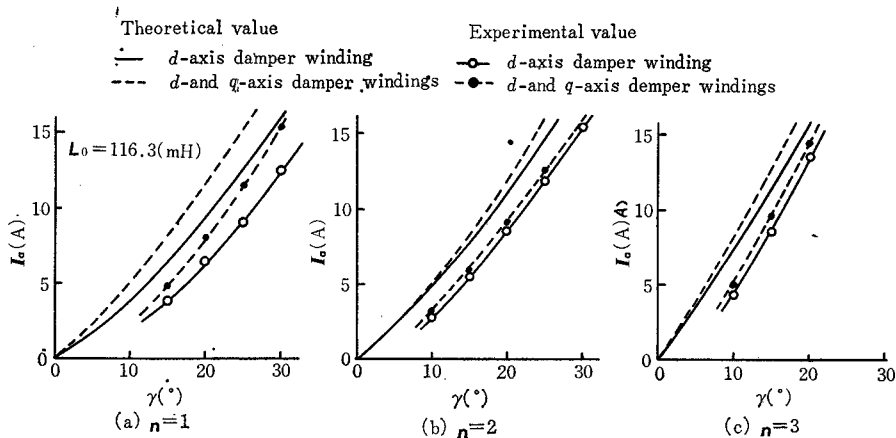


Fig. 9. Allowable armature current limit  $v$ , s leading commutating angle.

difference from that for the  $d$ -axis damper winding, but for  $n=1$ , that difference becomes considerably large. From eqs. (8) and (9), the maximum over-lapping angle at which the allowable armature current limit is given is  $\gamma$ . Consequently, it is considered that the allowable armature current is effected with a mean inductance between  $\theta$  and  $\gamma$  in Fig. 6. The difference of the mean inductance for  $n=2$  or 3 is slight, but for  $n=1$  that difference considerably large. These facts may be extended to the allowable armature current.

## 6. Conclusion

A summary of the results is shown below ;

(1) The field winding works as the effective  $d$ -axis damper winding and improves the commutation characteristics such as the over-lapping angle and the allowable armature current limit.

(2) The  $q$ -axis damper winding is able to decrease the armature inductance near the  $q$ -axis, so that the commutation characteristics become better for  $n=1$ , especially on the large commutation angle.

(3) But for  $n=2$  and 3, the commutation characteristics are hardly effected by the  $q$ -axis damper winding.

## References

- 1) S. Miyairi and Y. Tsunehiro, J. I. E. E. of Japan **87-8**, 947, 1601 (1967).
- 2) N. Sato, J. I. E. E. of Japan **91**, 6, 1065 (1971).
- 3) N. Sato and N. Yamaguchi, J. I. E. E. of Japan **93-B**, 1, 33 (1973).
- 4) S. Yasuoka, Y. Hayashi, Y. Takeda and T. Hirasa, Lecture G3-16 in Annual Meeting of Kansai Branch of I. E. E. of Japan (October 1973).
- 5) Y. Takeda and T. Hirasa, J. I. E. E. of Japan **93-B**, 2, 68 (1973).
- 6) S. Fukuda and H. Fujiwara, J. I. E. E. of Japan **92-B**, 9, 487 (1972).
- 7) H. Sasajima, T. Tsuchiya and M. Naito, J. I. E. E. of Japan **88-11**, 962, 2099 (1968).
- 8) T. Sato, Y. Tsunehiro and Y. Adachi, J. I. E. E. of Japan **91**, 8, 1479 (1971).